NANO LETTERS

Letter

pubs.acs.org/NanoLett

Enhancing Nanoparticle Electrodynamics with Gold Nanoplate Mirrors

Zijie Yan, Ying Bao, Uttam Manna, Raman A. Shah, and Norbert F. Scherer*

The James Franck Institute, The University of Chicago, 929 East 57th Street, Chicago, Illinois 60637, United States

Supporting Information

ABSTRACT: Mirrors and optical cavities can modify and enhance matter−radiation interactions. Here we report that chemically synthesized Au nanoplates can serve as micrometer-size mirrors that enhance electrodynamic interactions. Because of their plasmonic properties, the Au nanoplates enhance the brightness of scattered light from Ag nanoparticles near the nanoplate surface in dark-field microscopy. More importantly, enhanced optical trapping and optical binding of Ag nanoparticles are demonstrated in interferometric optical traps created from a single laser beam and its reflection from individual Au nanoplates. The enhancement of the interparticle force constant is ≈20-fold more than expected from the increased intensity due to standing wave interference. We show that the additional stability for optical binding arises from the restricted axial thermal motion of the nanoparticles that couples to and reduces the fluctuations in the lateral plane. This new mechanism greatly advances the photonic synthesis of ultrastable nanoparticle arrays and investigation of their properties.

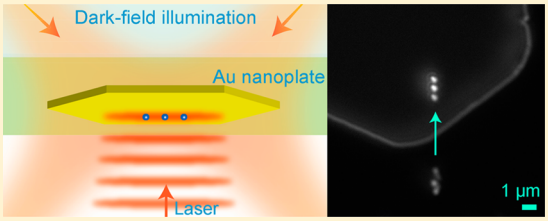

KEYWORDS: *Optical tweezers, optical manipulation, plasmonics, nanostructures*

Creating new types of optical components or imbuing traditional optics with new properties can enhance measurements and manipulation of nanoparticles and nanostructures. Mirrors, fabricated as layers of metallic or dielectric materials coated on substrates, are ubiquitous components of modern optical experiments, where they define laser cavities,[1] serve as essential elements for beam steering and beam shaping (e.g., spatial light modulators),[2,3] and play key roles in light-emitting and harvesting devices.[4,5] Plane mirrors are also useful in optical trapping; the normal reflection creates a counter-propagating beam geometry where the radiation pressure is nearly completely compensated in interferometric optical tweezers.[6] Also, the antinode along the propagation direction defines a narrow axial optical trapping region due to the steeper gradient compared to a conventional optical focus. It has been shown that interferometric trapping can significantly increase the axial trap stiffness,[7−9] making possible three-dimensional optical trapping and optical binding of even highly scattering and absorbing metal nanostructures.[10,11]

An ideal optic for interferometric applications would be one that enhances the electrodynamic properties of the nanomaterials being manipulated and studied and that actually serves to enhance the detection conditions so that smaller objects can be studied. For example, extraordinary optical transmission, discovered by Ebbesen,[12] involves enhanced transmission of light in noble metal mirrors with submicrometer size holes. The holes facilitate plasmon excitation by light onto the incident surface, plasmon coupling from one surface to the other, and the coupling from the distal surface to free space radiation by way of symmetry breaking; otherwise, plasmon excitation is impossible due to the infinite planar nature of the metal film and the dispersion relation this creates.[13−15]

Here we show that chemically synthesized Au nanoplates can serve as transmissive mirrors that enhance optical detection and electrodynamic interactions. The recent development of a polyol method has made the synthesis of high-quality Au nanoplates straightforward.[16−18] The single-crystalline Au nanoplates have atomically flat surfaces over micrometer length scales,[18,19] creating "perfect" mirrors to reflect (near-)infrared laser beams with negligible distortion. We demonstrate enhanced optical trapping and optical binding of Ag nanoparticles in interferometric optical traps created by the Au nanoplate mirrors. Moreover, the Au nanoplates, which are >100 nm thick (i.e., far beyond the penetration depth of visible light in Au), exhibit a type of "extraordinary luminosity" that enhances the imaging of other objects, such as Ag nanoparticles, that are positioned in front of the Au nanoplate. The nanoparticles look even brighter compared to the same particles positioned over a transparent cover glass adjacent to the Au nanoplate mirror.

The experiments were performed with an optical tweezers apparatus.[20] Specifically, a linearly polarized Gaussian beam with λ = 800 nm (vacuum wavelength hereafter) from a Ti:sapphire laser was shaped by a spatial light modulator to generate structured optical beams, including optical lines and Bessel beams. The laser power was 60 mW at the back aperture of the objective (Olympus UPLSAPO, 60× water immersion,

Received: January 9, 2014
Revised: March 31, 2014
Published: April 17, 2014

   dx.doi.org/10.1021/nl500107w | *Nano Lett.* 2014, 14, 2436−2442

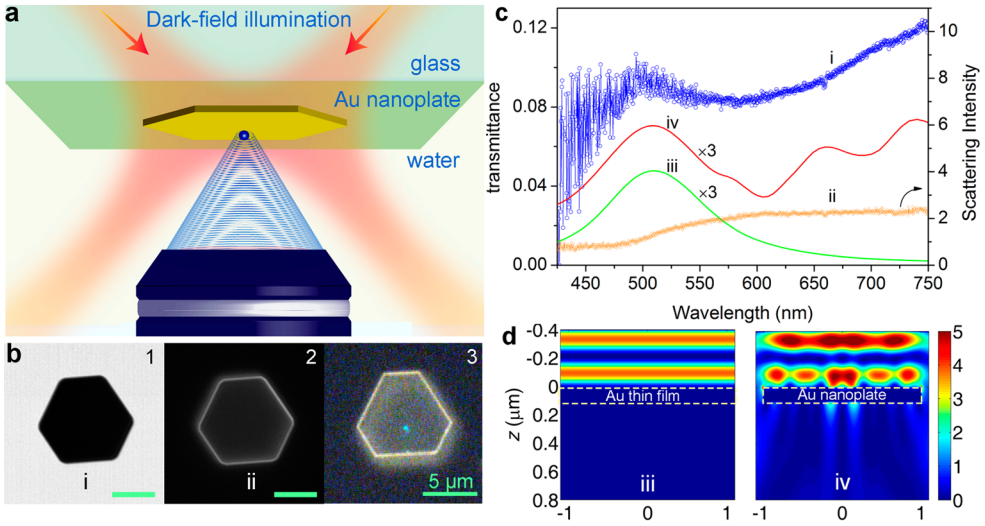

Figure 1. Extraordinarily transmissive gold nanoplates under dark-field microscopy. (a) Schematic of the dark-field microscopy configuration. (b) Bright-field (b-1) and dark-field (b-2,3) optical images of Au nanoplates. Note that b-3 is a true color (RGB) image, in which a single 100 nm diameter Ag nanoparticle (blue dot) was trapped by an optical line trap near the Au nanoplate surface. (c) i. Transmission spectrum of the central area of the Au nanoplate in b-1 (without any nanoparticle) obtained in bright-field microscopy. ii. Scattering spectrum of the same area in b-2 obtained by dark-field microscopy. iii. Transmission spectrum of an infinitely large Au thin film of 100 nm thickness at a glass/water interface calculated by FDTD simulations. iv. Calculated (FDTD) transmission spectrum of a 100 nm thick Au nanoplate from the top. (d) Calculated intensity distributions of electric fields (normalized to the incident fields) around the Au thin film and nanoplate illuminated by a plane wave at λ = 700 nm. Details of the simulations are presented in the Supporting Information, Figure S3.

NA 1.2). Au nanoplates were synthesized following a polyol process.[18] The products of the reaction include truncated triangles, hexagons, and irregular polygonal disks with sizes (the longest diagonals) up to 40 μm and thicknesses in the range of 100−600 nm (Supporting Information, Figure S1). An aqueous droplet of the Au nanoplates was dried on a coverslip allowing the Au nanoplates to adhere. This dilutely coated coverslip was then used to build a sample cell[20] containing an aqueous solution of Ag nanoparticles. Optical images were recorded with a high frame rate CMOS camera (Andor Neo). Alternatively, we could switch the imaging to another beam path in the microscope to simultaneously record RGB color images (with a Sony XCD-V60CR CCD) and scattering spectra (using an Andor Shamrock imaging spectrometer) of the same object.[20]

As depicted in Figure 1a, we focused a laser beam onto a nanoplate surface to generate an interferometric optical trap, and used dark-field microscopy for imaging. As shown in Figure 1b-1, all the Au nanoplates we studied appear black (opaque) under bright-field microscopy (with a NA = 0.9 bright field condenser). This follows by considering the skin depth of Au[21]

$$\delta(\omega) = \frac{\sqrt{2}\,c}{\omega}\left[\sqrt{\varepsilon_R(\omega)^2 + \varepsilon_I(\omega)^2} - \varepsilon_R(\omega)\right]^{-1/2} \quad (1)$$

where $\varepsilon_R(\omega)$ and $\varepsilon_I(\omega)$ are the real and imaginary parts of the dielectric function, respectively, ω is the angular frequency of the light, and c is the speed of light in vacuum. Using the Johnson and Christy (J−C) dielectric function for Au,[22] the calculated skin depth of Au is less than 50 nm in the visible spectrum (Supporting Information, Figure S2), much smaller than the thicknesses of the Au nanoplates (>100 nm). However, there is significant scattered light from the edges of the nanoplate in dark-field microscopy (Figure 1b-2).

More importantly, the same Au nanoplates bestow enhanced brightness to nanoparticles in dark-field images. A 100 nm Ag nanoparticle (diameter 99.0 ± 5.7 nm, polyvinylpyrrolidone coated, purchased from nanoComposix Inc.) can be clearly seen in front of a Au nanoplate in Figure 1b-3. In fact, since the same particle was trapped and moved over the nanoplate, we determined that it is brighter over the plate than over the coverslip! This is a surprising observation considering that the illumination was from the backside of the Au nanoplate in our optical setup, as illustrated in Figure 1a. Since the plate thickness > skin depth, little illumination light should be able to penetrate the Au nanoplate and reach the Ag nanoparticle. Even more interestingly, the enhanced brightness of the trapped and dragged nanoparticle does not occur only at the edge of the plate but essentially everywhere the particle is moved.

We measured the transmittance near the central area of the Au nanoplate in bright field (Figure 1b-1) and the scattering intensity of the same area in dark field (Figure 1b-2); the results are shown in Figure 1c as curves i and ii, respectively. Note that the scattering intensity is normalized with the formula $I_{scat} = (I_{obj} - I_{ref})/I_{ref}$, where I_{obj} is the recorded scattering intensity from an area of interest and I_{ref} is the scattering intensity from the equivalent size region of a coverslip. The transmittance is generally <0.12 for visible light and the measured transmittance is significantly enhanced on the red side of the spectrum. The measured transmittance from the Au nanoplate has a very different spectral shape and is greater than that of a 100 nm thick Au thin film (curve iii) calculated via finite-difference time-domain (FDTD) simulations performed using Lumerical "FDTD Solutions" software using the J-C data.[22]

It is known that Au thin films can support surface plasmon polaritons (SPPs), but free space EM radiation cannot couple into SPPs in a thin film due to the momentum mismatch. However, symmetry breaking at the edges of nanoplates relaxes the strict momentum matching constraint for launching SPPs.[17] In Supporting Information Figure S4, we demonstrate that when a laser beam is focused at the edges of a Au nanoplate, SPPs can be excited and propagate along the surface of the

dx.doi.org/10.1021/nl500107w | Nano Lett. 2014, 14, 2436−2442

nanoplate, while this does not happen when the laser is focused in the central area. The simulation results shown in Figure 1d demonstrate the importance of the nanoplate edges; SPP excitations are launched in a Au nanoplate but not in an extended thin film. When the Au thin film is replaced by a hexagonal nanoplate, the calculated transmittance is increased throughout the visible (Figure 1c, curve iv), especially at red and near-IR wavelengths. This agrees well with the measured spectrum. We note that the light source in the simulation has normal incidence to the Au nanoplate, but the light focused by a high NA condenser illuminates the nanoplate from a large angle that promotes the excitation of SPPs. (In the simulation, large angles of illumination cause numerical errors so we chose normal incident angles for accuracy.) This difference is the most likely source of discrepancy for the magnitude of the measured vs calculated transmittance. Nevertheless, these results show that the enhanced transmittance is related to the SPPs of the Au nanoplates.

The SPPs launched in this way, in turn, can couple to localized surface plasmons (LSPs) in a nearby nanoparticle. As a result, the Au nanoplate can function as an "extraordinarily transmissive" illumination source for optically trapped Ag nanoparticles. The SPPs excited in Au nanoplates are similar to the focusing of SPPs by circular and elliptical structures milled through an optically thick metallic film[23] or by a Au thin film illuminated by a radially polarized laser beam.[24] We checked the brightness of a trapped nanoparticle at different positions away from the edges but did not find obvious differences (Supporting Information, Figure S5). This is because the illumination for imaging was from an incoherent white light source (i.e., a tungsten halogen lamp) whose spatial coherence length is much smaller than the nanoplate size. Therefore, the nanoplate does not have structured SPP interference as the simulations performed with spatially and temporally coherent illumination suggest.[25] However, it should with spatially coherent illumination.

Figure 2a illustrates how interferometric optical tweezers are created using a Au nanoplate. When a laser beam impinges at normal incidence on an optically thick Au nanoplate, the Au nanoplate behaves as a mirror and reflects the beam back, forming a standing wave pattern along the beam propagation direction due to interference. Figure 2b shows the calculated standing wave from an 800 nm (vacuum wavelength) incident beam. The good near-IR reflectivity (>95%) (Figure 2c) and plasmonic properties of Au nanoplates make them good micrometer-size mirrors to construct interferometric optical tweezers while still enabling dark-field imaging of the trapped objects. Consequently, we can use a single Au nanoplate to build interferometric optical tweezers and thus enhance optical trapping of very small nanoparticles. Figure 2d shows 3D optical trapping of a 30 nm Ag nanoparticle (diameter 30.7 ± 3.3 nm, citrate coated, produced by thermal reduction of $AgNO_3$ with citrate[26]) with an interferometric Fourier-transformed Bessel beam (IFTB) trap using a Au nanoplate (image 1). The trapping stability is better when a nanoparticle is trapped closer to the nanoplate due to the finite nondiffracting length of the IFTB beam.[10] However, to demonstrate the impressive optical trapping stability, we show an example of trapping 4 μm away from the plate surface. At larger separations the reflected IFTB beam starts to spread out (i.e., after a propagation length of 8 μm). At a 4 μm distance, the Ag nanoparticle could be stably trapped for over 10 min and be moved around as long as the Bessel beam was incident on the

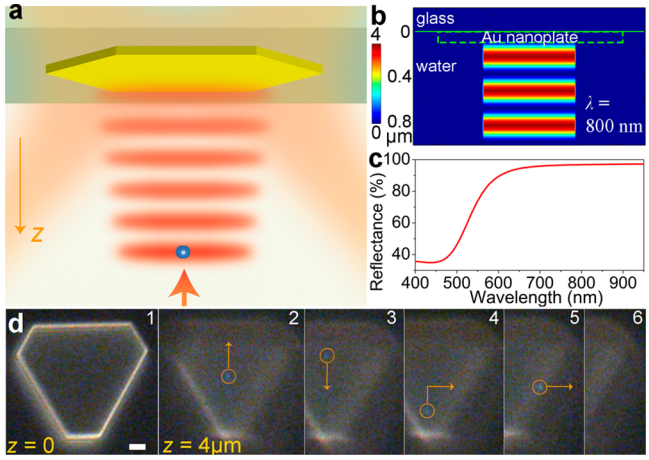

Figure 2. Interferometric optical tweezers constructed with a single Au nanoplate. (a) Schematic of using a Au nanoplate as a mirror to construct interferometric optical tweezers. (b) Calculated intensity distribution of a standing wave formed by a 800 nm plane wave incident on the central area of the Au nanoplate. (c) Calculated reflectivity of the central area of a 100 nm thick Au nanoplate. (d) Experimental demonstration of 3D optical trapping of a 30 nm Ag nanoparticle with an interferometric Fourier-transformed Bessel beam (IFTB) trap (see Supporting Information, Video S1). The trap was constructed by interfering a Fourier-transformed Bessel beam with its own reflection from a Au nanoplate (image d-1). Note that the focal planes of both the imaging and trapping systems were fixed at $z = 0$, so when the nanoplate was moved to $z = 4$ μm, the trapped nanoparticles would be 4 μm away from the plate surface (images 2–5). The nanoparticle was well trapped everywhere over the nanoplate. Once the Ag nanoparticle was moved off the Au nanoplate, it could not be trapped (image 6). The white scale bar is 1 μm.

Au nanoplate (images 2–5; also see Supporting Information, Video S1). In contrast, the nanoparticle escaped when it was moved past the edge of the Au nanoplate (image 6), demonstrating the important role of the Au nanoplate for enhanced trapping.

The Au nanoplates also enhance the optical binding of (i.e., the electrodynamic interactions between) nanoparticles. In Figure 3a, three Ag nanoparticles (100 nm diameter) were first confined near a glass surface by a line trap and then moved over a Au nanoplate (see Supporting Information, Video S2). The line trap was ~7 μm long (at the 10% value of maximum intensity) and diffraction-limited (~300 nm fwhm) in width. Its long axis was along the y-axis (lab frame) and linear polarization was along the x-axis. This "perpendicular" configuration facilitates optical binding.[27] Near the glass surface, the optical binding interactions between the three Ag nanoparticles were weak, as manifested by their broad position distributions (Figure 3b-I). However, when the same nanoparticles were moved and positioned over the Au nanoplate surface, the optical binding interactions were tremendously enhanced; the three nanoparticles became a nearly rigid body with strongly correlated motions (Figure 3b-II) despite the random thermal energy (k_BT) of each Ag nanoparticle. As an example, Figure 3c shows representative histograms of the separations between two Ag nanoparticles near the coverslip and the same particles over a Au nanoplate. It is obvious that the fluctuations of interparticle separation are much less over the Au nanoplate. This is a general behavior that occurs for various groups of nanoparticles.

dx.doi.org/10.1021/nl500107w | Nano Lett. 2014, 14, 2436–2442

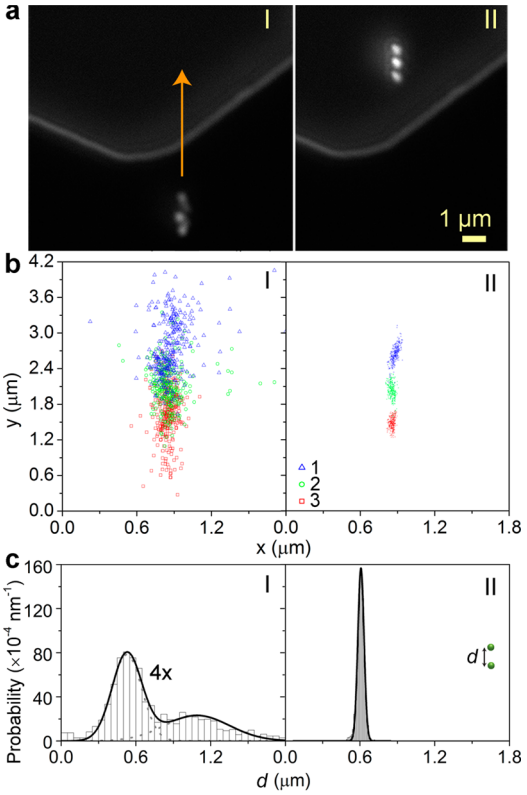

Figure 3. Significantly enhanced optical binding of Ag nanoparticles over a Au nanoplate. (a) Optical images of three Ag nanoparticles (100 nm diameter) confined by an optical line trap (I) near a coverslip and (II) near a Au nanoplate surface (Supporting Information, Video S2). The line trap is along the *y*-axis with the direction of linear polarization along the *x*-axis. (b) The corresponding position distributions of the nanoparticles (50 fps for 6 s). (c) Representative histograms of the interparticle separations between two Ag nanoparticles near the coverslip glass or a Au nanoplate surface. The data in panel 1 (left) has been multiplied by 4 to allow visualizing the shape of the distribution. The solid curves are Gaussian fits. Note that the fitted curve in the top panel shows a second peak at ~1.1 μm, which is the second optical binding position ($\sim 2\lambda/n$ for 800 nm light in water; n = 1.33).

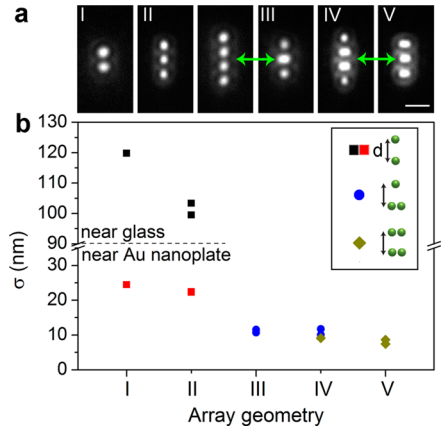

Figure 4. Optical binding geometries and stabilities of Ag nanoparticles over a Au nanoplate. (a) Optical images of arrays of Ag nanoparticles (100 nm diameter) formed near a Au nanoplate surface. Note that in geometries III–V, the brighter central features are actually dimers stabilized by optical trapping interactions and repulsive electrostatic interactions (Supporting Information, Video S3). The scale bar is 1 μm. (b) Standard deviations (σ) of the separations (d) between adjacent Ag nanoparticles or clusters in arrays of different geometries obtained from distributions like those shown in Figure 3b. Three types of adjacent Ag nanoparticles or clusters can be identified in these arrays as illustrated in the legend, where the closely packed green spheres along the *x*-axis represent the dimers. Multiple points (symbols) are shown for III–V that represent the standard deviations of particular interactions in the multiparticle clusters (see legend).

The enhanced optical binding by Au nanoplate mirrors greatly facilitates the creation of stable chains or arrays of Ag nanoparticles. Typical optical binding geometries obtained near a Au nanoplate are shown in Figure 4a. Note that when there were four or more Ag nanoparticles, they tended to form arrays with spacings characteristic of near-field and optical binding interactions rather than single chains near the Au nanoplate. By contrast, when near the coverslip the same nanoparticles fluctuated greatly in interparticle separation without forming rigid chains or arrays. Figure 4b summarizes the standard deviations of the fluctuations between adjacent Ag nanoparticles or clusters in arrays of different geometries. It is clear that the Au nanoplate mirror significantly increases the stability of the chains or arrays of Ag nanoparticles as the fluctuations of interparticle separations decrease by ~5 times (i.e., nanoplate vs glass coverslip). In addition, arrays with two nanoparticles in the same optical binding site appeared to be more stable; the two nanoparticles could be regarded as a near-field bound cluster (e.g., near-field dimer) with a larger scattering cross section that further increases the optical binding forces.

In addition to the large enhancement of optical binding, we also find that the Ag nanoparticles became much brighter near the Au nanoplate surface (Figure 3a). Scattering from the nanoparticles increases when they are over the Au nanoplate even though light transmission through the nanoplate was much lower than through the coverslip. The increased scattering results from the presence of SPPs launched in the Au nanoplate; the Ag nanoparticles are able to scatter the evanescent field associated with the SPPs into free space. Although the separation of interference fringes is 300 nm in our case (i.e., half the wavelength in the medium), the distance between the first fringe and the nanoplate surface is only ~120 nm (see Figure 2b and Supporting Information, Figure S6). This is due to light propagation and reflection from the finite skin depth of the nanoplate (e.g., ~26 nm at λ = 800 nm). With diameters of 100 nm, the gap between the trapped Ag nanoparticles and the Au nanoplate will be ~75 nm, which is in the near field of the Au nanoplate (see Figure 1d). Coupling between a LSP in a metal nanoparticle and an SPP in a thin metal film separated by gaps of tens of nanometers has been theoretically predicted,[28] and the resultant increase in the far-field scattering from the nanoparticle near the metal film has been experimentally demonstrated.[29]

We tested this LSP–SPP coupling for the present experiment by measuring the scattering spectra.[28,29] We measured the scattering spectra of a single Ag nanoparticle with and without a Au nanoplate (see Supporting Information, Video S4). In Figure 5a, a 100 nm Ag nanoparticle (i in panel 1) was first confined near the coverslip surface by a line trap and then moved over a Au nanoplate, where the nanoparticle appeared much brighter. The corresponding scattering spectra are shown in Figure 5b. It is clear that the scattering intensity of the Ag nanoparticle near the Au nanoplate surface (curve iii) is greater than that near the glass surface (curve i), and the spectrum is red-shifted. The measurements also address another factor that could have the appearance of making the nanoparticle look

dx.doi.org/10.1021/nl500107w | Nano Lett. 2014, 14, 2436–2442

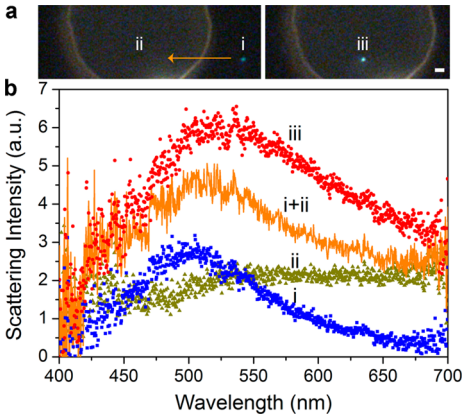

Figure 5. LSP−SPP coupling between a Ag nanoparticle and a Au nanoplate. (a) Dark-field optical images of a Au nanoplate and a Ag nanoparticle (100 nm diameter). Left: the particle i was held by an optical line trap near a coverslip surface. Right: the same particle (relabeled as iii) was moved laterally and positioned above the Au nanoplate surface (Supporting Information, Video S4). The white scale bar is 1 μm. (b) The corresponding scattering spectra of the nanoplate (curve ii) and nanoparticles (same i, iii as in panel a). The curve i + ii is the sum of curves i and ii; i.e., the linear combination of scattering intensity as a result of positioning the particle over the nanoplate.

brighter, that is, scattering from the Au nanoplate that was added to the scattering (spectrum) of the Ag nanoparticle. Figure 5b shows that the measured scattering intensity (curve iii) is stronger than the sum of the scattering intensity of the nanoparticle and the background intensity of the Au nanoplate (curve i + ii), and the scattering in curve iii is significantly enhanced on the red side of the spectrum. The difference (amplitude and discernible red-shift) between curve iii and i + ii indicates the effect of the nanoplate mirror and its coupling with the optically trapped Ag nanoparticle. The measured red-shifted (and enhanced) spectra are consistent with plasmonic coupling between metal nanoparticles and films.[28,29]

We now consider the cause of enhancement of optical binding. One factor is the increase of the optical field intensity due to interference. When positioned over the Au nanoplate, the optical line trap forms a standing wave in the axial direction so the nanoparticles are trapped by a constructive interference fringe.[11] Since the confocal parameter for the line trap is short, this effect is predominantly in the first few antinodes near the nanoplate surface, as shown in Figure 2b. Simple superposition implies a doubling of the electromagnetic fields at the antinodes and hence a factor of 4 enhancement in the intensity (shown in red). Since optical binding forces scale linearly with the field intensity,[20,27] one would expect the optical binding to be more stable near a Au nanoplate. However, the measured enhancement is much larger than this simple estimate allows. The spring constant, κ, of optical binding scales linearly with the optical field intensity, and from the equipartition theorem,[11,30] $\kappa^{-1} \propto \sigma^2$; i.e., stiffness is inversely proportional to the variance of the position. Therefore, a 4-fold increase of κ should result in a 2-fold decrease of σ, but the data plotted in Figure 4 show a ~5-fold decrease of σ.

It was suggested that the close proximity to the mirror surface allows new paths for light to scatter from particle to particle; i.e., by way of reflection from the mirror.[11] In our case, the location of the metal nanoparticle is ~120 nm above the mirror, which makes this putative path ~650 nm vs ~600 nm center-to-center. However, the reflection from the mirror gives a π phase shift so that there could actually be a reduction in field amplitude at each particle due to partial destructive interference. In fact, our FDTD simulations for two-particle optical binding (Supporting Information, Figure S6) indicate that increases of the intensity in the antinode is <4-fold, giving a <2-fold reduction of σ, so this proposed mechanism is not operative. The additional reduction of σ in our measurements does not arise from additional field enhancements beyond what is observed from standing wave interference. Another possibility is the plasmonic coupling between the Ag nanoparticles and the Au nanoplate in the intense optical trapping field,[31] yet this coupling is not evident in our simulations (Supporting Information, Figure S6). As a control experiment, we studied the optical binding of Ag nanoparticles over a regular dielectric mirror (Supporting Information, Figure S7) and found that the optical binding of two or three Ag nanoparticles has similar stability as that over the Au nanoplates, further indicating that the plasmonic coupling does not play a significant role in enhancing the optical binding.

We are only able to observe motion in two Cartesian directions with high resolution (nm scale). If there is an electrodynamically induced mechanical coupling between different Cartesian degrees of freedom, then the significantly enhanced optical binding could result from the increased axial trap stiffness due to the standing wave trapping configuration. It has been shown theoretically that the strong modulation of the axial intensity due to interference can increase the axial trap stiffness of submicrometer particles in a standing wave optical trap by at least 2 orders of magnitude over that in a single beam optical trap.[8,9] Therefore, the axial fluctuations of the Ag nanoparticles over the Au nanoplates would be (at least) an order of magnitude smaller than over the transparent glass since $\kappa^{-1} \propto \sigma^2$.[11,31]

Indeed, as shown in Figure 6, optical binding depends nontrivially on the axial configuration. The curves of z−x coupling were obtained by FDTD simulations with the configuration illustrated in the bottom-left inset of Figure 6a. Introducing a small relative displacement in z (labeled Δz separation) reduces the equilibrium separation of the particles in the x-direction. In other words, the axial fluctuation is coupled to the transverse fluctuation via electrodynamic interactions; the coupling has a slope = −1 as shown in Figure 6b. Since our measurements are in a thermal environment, random forces are always acting to cause Brownian motion. A suppression of metal nanoparticle motion along the axial direction in a standing wave optical trap will also reduce the relative particle motions in the x−y plane (i.e., the coordinates we measure). Therefore, the thermal fluctuations will be significantly suppressed when the nanoparticles are trapped over a Au nanoplate in an interferometric trap. As a result, the measured variance decreases by an additional amount (or the interparticle potential of mean force increases) by this z−x coupling, and the observed optical binding of Ag nanoparticles over a Au nanoplate becomes much more stable as shown in Figures 3 and 4. In fact, we estimate that the standard deviation of z-axis fluctuations for k_BT energy is ~20 nm (Supporting Information, Figure S8), and this stability is conferred to the x-axis interparticle separation. Together with the field enhancement due to interference, this new mechanism accounts well for the decrease of the variances shown in Figure 4.

We have shown that Au nanoplates can serve as extraordinarily transmissive field-enhancing mirrors that vastly

dx.doi.org/10.1021/nl500107w | Nano Lett. 2014, 14, 2436−2442

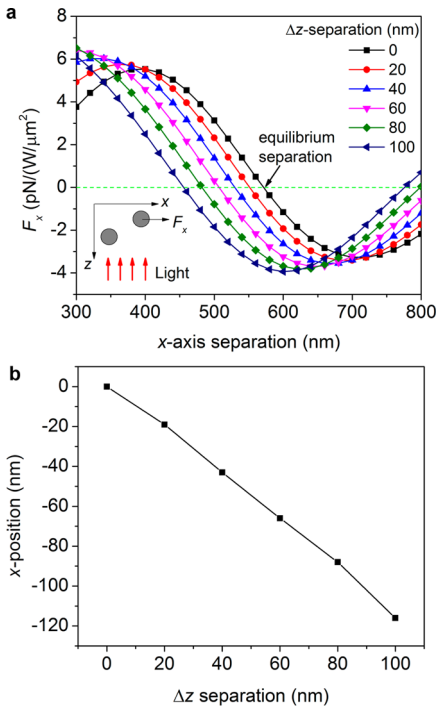

Figure 6. Electrodynamic coupling of nanoparticle motions via optical binding interactions. (a) Calculated interparticle forces of two Ag nanoparticles (diameter 100 nm) with different separations along the *x*- and *z*-directions; their *y*-positions are the same. The optical forces are calculated by integrating the Maxwell stress tensor over a surface surrounding the nanoparticle. We assume the particles are in a dielectric of water and illuminated by a λ = 800 nm (vacuum wavelength) plane wave that is linearly polarized along the *y*-axis. (b) Change of the equilibrium separation along the *x*-axis when the two nanoparticles have different *z*-axis separations (Δz).

improve electrodynamics and optical trapping experiments. Enhanced optical trapping and optical binding of Ag nanoparticles are demonstrated by constructing interferometric optical traps from a single laser beam using a single Au nanoplate. The finite-size Au nanoplate mirror makes the demonstration of these enhancements possible for identical nanoparticles since we can drag the particles from regions over glass to regions over the mirror, which would be impossible with a macroscopic mirror unless it has a sharp edge. The enhancements reveal the electrodynamic coupling of particle motions in three dimensions via optical binding interactions, which we believe have not been considered before. The suppressed fluctuations in the axial (z) direction affect the fluctuations in the transverse direction parallel to the plate and plane of interference (x, y). We also found interesting optical properties of the Au nanoplates in dark-field microscopy, where they behave analogously to extraordinarily transmissive substrates that improve the imaging of Ag nanoparticles near the nanoplate surfaces by enhancing the scattering of light from nanoparticles that are in close proximity (~100 nm) to the Au nanoplate.

The unique properties of Au nanoplates make them attractive platforms for optical manipulation and detection of nano-objects and perhaps biomolecules. For example, the Au nanoplates will enable constructing interferometric tweezers for trapping whole cells and even tissue slices. The IFTB trap used here would ameliorate the beam distorting effects of scattering media due to the non-diffracting and self-healing properties of Bessel beams. These advances could improve optical diagnostics and optical surgery in live cells.[32] Also, the mirror geometry can be used to create 3D arrays of optically bound metal nanoparticles that would have novel photonic properties and large field enhancements for co-trapping[33] as well as applications in quantum optics.

■ ASSOCIATED CONTENT

Supporting Information

Movie clips showing the optical manipulation processes and additional figures. This material is available free of charge via the Internet at http://pubs.acs.org.

■ AUTHOR INFORMATION

Corresponding Author

*E-mail: nfschere@uchicago.edu (N.F.S.).

Author Contributions

Y.B. and U.M. contributed equally to this work. Z.Y. and N.F.S. designed the research and wrote the manuscript. Z.Y. performed the experiments and numerical simulations. Y.B. synthesized the Au nanoplates, U.M. contributed to the spectroscopy measurements, and R.A.S. contributed to the analysis of the mechanism of enhanced optical binding.

Notes

The authors declare no competing financial interest.

■ ACKNOWLEDGMENTS

This work was supported by the National Science Foundation (CHE-1059057). We also used the University of Chicago NSF-MRSEC (DMR-0820054) central facilities. We thank Dr. Matthew Pelton and Dr. Stephen Gray for helpful discussions.

■ REFERENCES

(1) Keller, U. *Nature* **2003**, *424*, 831−838.
(2) Igasaki, Y.; Li, F. H.; Yoshida, N.; Toyoda, H.; Inoue, T.; Mukohzaka, N.; Kobayashi, Y.; Hara, T. *Opt. Rev.* **1999**, *6*, 339−344.
(3) Thomson, R. R.; Bockelt, A. S.; Ramsay, E.; Beecher, S.; Greenaway, A. H.; Kar, A. K.; Reid, D. T. *Opt. Express* **2008**, *16*, 12786−12793.
(4) Nishimura, S.; Abrams, N.; Lewis, B. A.; Halaoui, L. I.; Mallouk, T. E.; Benkstein, K. D.; van de Lagemaat, J.; Frank, A. J. *J. Am. Chem. Soc.* **2003**, *125*, 6306−6310.
(5) Lin, C. L.; Lin, H. W.; Wu, C. C. *Appl. Phys. Lett.* **2005**, *87*, 021101.
(6) Ashkin, A. *Phys. Rev. Lett.* **1970**, *24*, 156.
(7) Zemanek, P.; Jonas, A.; Sramek, L.; Liska, M. *Opt. Lett.* **1999**, *24*, 1448−1450.
(8) Trojek, J.; Karasek, V.; Zemanek, P. *Opt. Express* **2009**, *17*, 10472−10488.
(9) Zemánek, P.; Jonáš, A.; Jákl, P.; Ježek, J.; Šerý, M. r.; Liška, M. *Opt. Commun.* **2003**, *220*, 401−412.
(10) Yan, Z.; Jureller, J. E.; Sweet, J.; Guffey, M. J.; Pelton, M.; Scherer, N. F. *Nano Lett.* **2012**, *12*, 5155−5161.
(11) Demergis, V.; Florin, E.-L. *Nano Lett.* **2012**, *12*, 5756−5760.
(12) Ebbesen, T. W.; Lezec, H. J.; Ghaemi, H. F.; Thio, T.; Wolff, P. A. *Nature* **1998**, *391*, 667−669.
(13) Pendry, J. B.; Martin-Moreno, L.; Garcia-Vidal, F. J. *Science* **2004**, *305*, 847−848.
(14) Martin-Moreno, L.; Garcia-Vidal, F. J.; Lezec, H. J.; Pellerin, K. M.; Thio, T.; Pendry, J. B.; Ebbesen, T. W. *Phys. Rev. Lett.* **2001**, *86*, 1114−1117.
(15) Chang, S. H.; Gray, S. K.; Schatz, G. C. *Opt. Express* **2005**, *13*, 3150−3165.
(16) Liu, H.; Yang, Q. *CrystEngComm* **2011**, *13*, 2281−2288.

(17) Major, T. A.; Devadas, M. S.; Lo, S. S.; Hartland, G. V. *J. Phys. Chem. C* **2013**, *117*, 1447−1452.
(18) Lee, J.-H.; Kamada, K.; Enomoto, N.; Hojo, J. *Cryst. Growth Des.* **2008**, *8*, 2638−2645.
(19) Huang, J.-S.; Callegari, V.; Geisler, P.; Bruening, C.; Kern, J.; Prangsma, J. C.; Wu, X.; Feichtner, T.; Ziegler, J.; Weinmann, P.; Kamp, M.; Forchel, A.; Biagioni, P.; Sennhauser, U.; Hecht, B. *Nat. Commun.* **2010**, *1*, 150.
(20) Yan, Z.; Shah, R. A.; Chado, G.; Gray, S. K.; Pelton, M.; Scherer, N. F. *ACS Nano* **2013**, *7*, 1790−1802.
(21) Park, T.-H.; Mirin, N.; Lassiter, J. B.; Nehl, C. L.; Halas, N. J.; Nordlander, P. *ACS Nano* **2008**, *2*, 25−32.
(22) Johnson, P. B.; Christy, R. W. *Phys. Rev. B* **1972**, *6*, 4370−4379.
(23) Liu, Z. W.; Steele, J. M.; Srituravanich, W.; Pikus, Y.; Sun, C.; Zhang, X. *Nano Lett.* **2005**, *5*, 1726−1729.
(24) Min, C.; Shen, Z.; Shen, J.; Zhang, Y.; Fang, H.; Yuan, G.; Du, L.; Zhu, S.; Lei, T.; Yuan, X. *Nat. Commun.* **2013**, *4*, 2891.
(25) Fu, Y.; Zhou, X. *Plasmonics* **2010**, *5*, 287−310.
(26) Wan, Y.; Guo, Z. R.; Jiang, X. L.; Fang, K.; Lu, X.; Zhang, Y.; Gu, N. *J. Colloid Interface Sci.* **2013**, *394*, 263−268.
(27) Dholakia, K.; Zemánek, P. *Rev. Mod. Phys.* **2010**, *82*, 1767−1791.
(28) Leveque, G.; Martin, O. J. F. *Opt. Express* **2006**, *14*, 9971−9981.
(29) Mock, J. J.; Hill, R. T.; Degiron, A.; Zauscher, S.; Chilkoti, A.; Smith, D. R. *Nano Lett.* **2008**, *8*, 2245−2252.
(30) Neuman, K. C.; Block, S. M. *Rev. Sci. Instrum.* **2004**, *75*, 2787−2809.
(31) Esteban, R.; Borisov, A. G.; Nordlander, P.; Aizpurua, J. *Nat. Commun.* **2012**, *3*, 825.
(32) Zhong, M.-C.; Wei, X.-B.; Zhou, J.-H.; Wang, Z.-Q.; Li, Y.-M. *Nat. Commun.* **2013**, *4*, 1768.
(33) Yan, Z. J.; Manna, U.; Qin, W.; Camire, A.; Guyot-Sionnest, P.; Scherer, N. F. *J. Phys. Chem. Lett.* **2013**, *4*, 2630−2636.